The 9th European Congress on Computational Methods in Applied Sciences and Engineering
ECCOMAS Congress 2024
3 – 7 June 2024, Lisboa, Portugal

NUMERICAL ANALYSIS OF DIFFERENT SEISMIC ISOLATION SYSTEMS

KAI GUO*, GABRIELE MIALNI†

* Department of Architecture, Built Environment and Construction Engineering (DABC)
Politecnico di Milano
Campus Leonardo, 20133 Milan, Italy
e-mail: kai.guo@polimi.it

† Department of Architecture, Built Environment and Construction Engineering (DABC)
Politecnico di Milano
Campus Leonardo, 20133 Milan, Italy
e-mail: gabriele.milani@polimi.it

Abstract: In the isolation at the base, the following devices are commonly used: lead rubber bearings (LRBs), high damping rubber bearings (HDRBs) and fiber reinforced elastomeric isolators (FREIs). Considering the high production cost and the difficult installation of the aforementioned devices, in this paper a novel seismic isolator including a classic isolator coupled with S-shaped steel dampers (SSSDs) is proposed and compared with conventional isolation devices. Suitable numerical models of seismic isolation devices are established in ABAQUS to identify the differences in terms of response. By discretizing the device into finite elements, the mechanical performance of the different isolation devices is investigated in terms of horizontal stiffness and damping capacity. The seismic isolator with SSSDs exhibits good dissipation performance, similar to that of the lead rubber bearing. Moreover, the low cost and easy installation of seismic isolators with SSSDs can be effectively applied in the structures instead of a traditional isolation system.

Key words: Finite Element Method, Seismic Isolation System, Effective Horizontal Stiffness, Damping Ratio.

1 INTRODUCTION

The traditional isolation systems commonly applied in engineering practice, consist in the majority of the cases of Nature Rubber (NR) Isolators, Lead Rubber Bearings (LRBs) and High Damping Rubber Bearings (HDRBs) [1]. Such conventional isolation systems generally improve the structural period and isolate seismic energy, especially in earthquake-prone areas.

Some novel hybrid systems recently proposed exhibit an improvement of the energy dissipation ability and of the damping ratio. For instance, there are seismic isolators coupled with shape memory alloy (SMA) wires [2], friction yield elastomeric bearings (FYEBs) [3], and slit steel rubber bearings (SSRBs) [4]. In a hybrid isolation system combining isolation and dissipation devices [5], [6], the system has good performance in terms of both energy dissipation and isolation capacities, significantly reducing displacements and accelerations.

Basing on a discretization obtained by means of the finite element method, a 3D model of a novel hybrid seismic isolator (NHSI) including a seismic isolator (SI) and S-shaped steel dampers (SSSDs) disposed in parallel is simulated in ABAQUS. This model is compared with traditional isolators, such as a classic Seismic Isolator (SI) and a Lead Rubber Bearing (LRB). The comparative analysis focuses on the mechanical properties of the three seismic isolators under constant vertical pressure and subjected to cyclic shear tests. In particular, the effective horizontal stiffness and the damping ratios are critically compared.

From simulations results, it is shown how the novel hybrid seismic isolator is more convenient than traditional seismic isolators, exhibiting enhanced energy dissipation and isolation capacities. In addition, it can be considered effective in significantly reducing potential earthquake damage.

The main objectives of the study are: (1) to evaluate the effectiveness of theoretical and numerical results; (2) to compare the performance of different types of isolators; (3) to investigate the effects of shape factor on different isolation systems.

2 THEORETICAL ANALYSIS

In engineering practice, seismic isolators are typically subjected to compression and shear forces. Based on the theory [7], [8], the mechanical capacities of the seismic system can be estimated and calculated using the formulas given in Eqs (1) - (5). The theoretical results are shown in Table 1.

$$\mathrm{K_h} = (\mathrm{F_{max}} - \mathrm{F_{min}})/(\Delta_{\mathrm{max}} - \Delta_{\mathrm{min}}) \tag{1}$$

$$\xi = \mathrm{W_d}/4\pi \mathrm{W_s} \tag{2}$$

$$\mathrm{W_s} = \frac{1}{2}\mathrm{K_h}\Delta_{\mathrm{ave}}^2 \tag{3}$$

$$\Delta_{\mathrm{ave}} = \frac{1}{2}(\Delta_{\mathrm{max}} + |\Delta_{\mathrm{min}}|) \tag{4}$$

$$T = 2\pi\sqrt{\frac{pA}{gK_h}} = 2\pi\sqrt{\frac{p}{g}\cdot\frac{t_r}{G}} \tag{5}$$

where $\mathrm{F_{max}}$, $\mathrm{F_{min}}$, Δ_{max} and Δ_{min} are the peak values of the horizontal force and displacement, respectively. $\mathrm{W_d}$ represents the dissipated energy (area within the loop), and $\mathrm{W_s}$ is the restored energy. p and A are the constant vertical pressure and the square area of the seismic isolator, respectively. Finally, the effective horizontal stiffness, horizontal period and damping ratio obtained from the 3D FE analyses of the three isolators are summarized and compared with the theoretical calculations.

Table 1. Theoretical calculation of seismic isolator.

Total thickness of rubber layer t_r (mm)	Total thickness of steel lamina t_s (mm)	Shape factor $S = \frac{a}{4t}$	Aspect ratio $R = \frac{a}{h}$	Pressure p (MPa)	Shear modulus G (MPa)	Horizontal period T_h (s)
50	2	3.75				0.869
48	4	3.91	2.88	3	0.8	0.852
46	6	4.08				0.834

3 NUMERICAL ANALYSIS

Potential isolators with different shape factors are considered to investigate the effects of shape factor on the mechanical behavior of the isolators, particularly in terms of damping ratio and effective horizontal stiffness.

The characteristics of the three potential isolators are shown in Figs. 1 - 3. It is noted that the NHSI and the LRB have similar effective horizontal stiffness and damping ratios; however, the NHSI has similar mechanical properties to the LRB and exhibits superior energy dissipation capacity compared to the SI.

To investigate the behavior of each isolator, 3D FE models are built and cyclic analyses are performed using ABAQUS software [9]. The isolators are subjected to cyclic shear tests at 0.5 Hz with maximum displacements of 50mm, 48mm and 46mm (corresponding to the total rubber thickness of the isolators) under a constant vertical pressure of 3 MPa.

3.1 Seismic isolator (SI)

The square SI consists of rubber layers and steel laminates. The rubber used is a standard type with a shear modulus of 0.8 MPa and a damping ratio of approximately 1%. A Yeoh model is adopted to represent the hyperelasticity of the rubber, while the damping behavior is described by the Prony series viscosity model. Comprehensive descriptions of the Yeoh hyperelasticity model and the Prony series viscosity model are provided in Tables 2 and 3, respectively.

The steel laminates are modeled using an isotropic-elastic behavior with Young's modulus of 206 GPa and Poisson ratio of 0.3. The steel laminates, made of common steel, have the yield strength of 345 MPa and the ultimate strength of 470 MPa.

The numerical model of the seismic isolator is established in ABAQUS in Fig. 1. In the seismic isolator, rubber pads are bonded to steel laminates, and the designed dimensions are 150×150×52 mm. The rubber material is modeled using eight-node linear brick with reduced integration and hybrid formulation (C3D8RH), while the steel material uses eight-node linear brick with reduced integration (C3D8R). The numerical results of the seismic isolator are presented in Table 4, showing that the horizontal periods of the seismic isolators with different shape factors are similar to theoretical results.

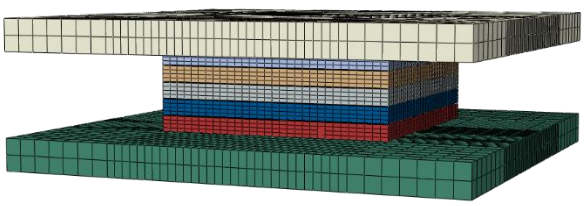

Figure 1. Mesh model of seismic isolator.

Table 2. Coefficients of the Yeoh hyperelastic model adopted in ABAQUS.

Type	C_{10}	C_{20}	C_{30}	D_1	D_2	D_3
Standard rubber	0.40746	0.0019039	0.000031585	0	0	0

Table 3. Coefficients of the Prony series model adopted in ABAQUS.

Type	g_1	τ_1	g_2	τ_2
Standard rubber	0.132	0.0203	0.207	8.03

Table 4. Data of seismic isolator in numerical model.

Total thickness of rubber layer t_r (mm)	Total thickness of steel lamina t_s (mm)	Shape factor	Horizontal stiffness K_h (N/mm)	Horizontal period T (s)	Damping ratio ξ
50	2	3.75	296.949	0.957	0.00938
48	4	3.91	311.912	0.934	0.00915
46	6	4.08	327.921	0.911	0.00896

3.2 Novel hybrid seismic isolator (NHSI)

Based on the mechanical properties of seismic isolators, a novel hybrid seismic isolator including seismic isolator and S-shaped steel dampers (SSSDs) is proposed and investigated. Unlike conventional seismic isolation systems that excel in energy isolation capacity, the inclusion of steel dampers in the novel hybrid system significantly enhances energy dissipation capacity.

The steel dampers are made of common steel with the Young Modulus of 206 GPa and the Poisson's ratio of 0.3. The FE models of SSSDs in Fig. 2 are built and simulated in ABAQUS [9]. SSSDs are bolted to upper and lower connection plates with dimensions of 150×40×2 mm, and consist of four straight parts and two semicircular parts, resembling bolted U-shaped steel dampers. In the numerical model, SSSDs are modeled using eight-node linear brick with reduced integration (C3D8R) element for the steel material, and the same element type as the rubber material used in the SI. The simulation results of the NHSIs with different shape factors are shown in Table 5.

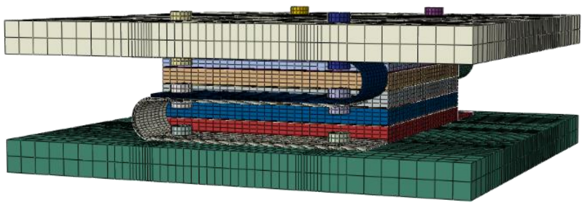

Figure 2: Mesh model of novel hybrid seismic isolator.

Table 5. Data of the novel hybrid seismic isolator in numerical model.

Total thickness of rubber layer t_r (mm)	Total thickness of steel lamina t_s (mm)	Shape factor	Horizontal stiffness K_h (N/mm)	Horizontal period T (s)	Damping ratio ξ
50	2	3.75	365.776	0.862	0.0906
48	4	3.91	380.754	0.845	0.0870
46	6	4.08	399.357	0.825	0.0860

3.3 Lead Rubber Bearing (LRB)

The LRB presented in Fig. 3, a commercial isolator applied in engineering practice, consists of a lead core with a diameter of 20mm as a dissipative device in addition to the rubber damping. Steel reinforcements are also required to improve the vertical stiffness of the bearing, as in the case of elastomeric isolators.

In this research, the LRB can be manufactured using the same materials as the SI, including rubber pads and steel laminates. The elastic-plastic behavior of the lead core significantly contributes to the total damping ratio of the LRB. The Young’s modulus and the yield strength of the lead core are set at 16 GPa and 14.4 MPa, respectively, with the Poisson ratio of 0.44. In FE model, the LRB has been simulated using eight-node linear brick with reduced integration (C3D8R) element for the lead core, and the same element types as those used for rubber and steel materials in the SI. The numerical results of the LRBs with different shape factors are presented in Table 6.

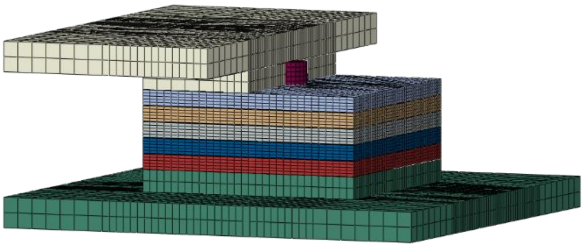

Figure 3: Mesh model of lead rubber bearing.

Table 6. Data of lead rubber bearing in numerical model.

Total thickness of rubber layer t_r (mm)	Total thickness of steel lamina t_s (mm)	Shape factor	Horizontal stiffness K_h (N/mm)	Horizontal period T (s)	Damping ratio ξ
50	2	3.75	338.575	0.896	0.0978
48	4	3.91	357.528	0.872	0.0960
46	6	4.08	378.354	0.848	0.0953

4 COMPARATIVE ANALYSIS

Figs. 4(a) to 4(c) present that the shear force - horizontal displacement curves obtained for the SI (red line), the LRB (black line) and the NHSI (blue line) under constant pressure and cyclic shear analysis.

The shear behaviors and stress distributions of different isolators under cyclic shear analyses are shown in Figs. 4 and 5. In the initial stage, with horizontal displacements equal to zero, the three isolators experience compressive deformations due to only constant vertical loads, leading to lateral deformations of the rubber pads. As the beginning of the cyclic shear analysis, the horizontal stiffness of the NHSI and the LRB is primarily attributed to the horizontal stiffness of steel dampers, SSSDs and the lead core. Once the steel dampers yield, the stiffness of the isolator mainly comes from the elastomer, which is much lower than the initial stiffness.

An elliptical hysteresis loop, which is the typical shear behavior of seismic isolator, is observed. The effective stiffness and damping of the isolators considering the shape factor effect, are computed at displacements of 50mm, 48mm and 46mm.

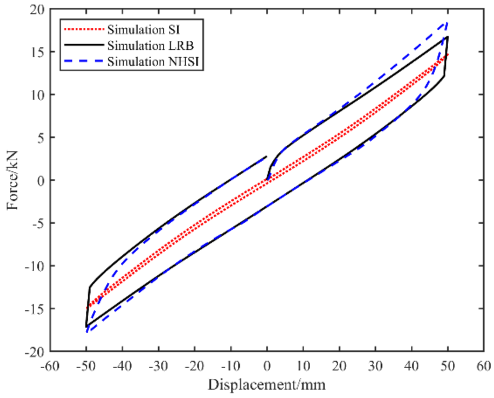

(a)

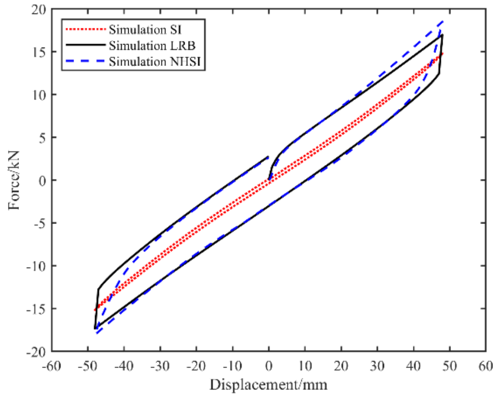

(b)

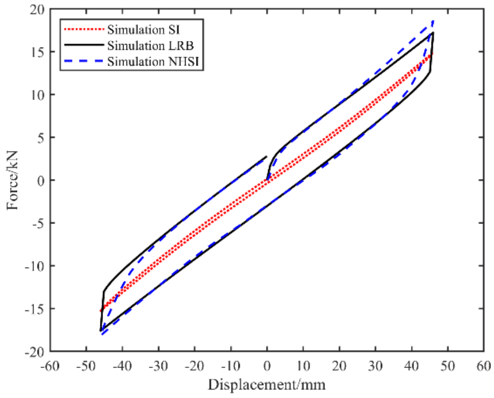

(c)

Figure 4: Comparative curves of different isolators with rubber thickness of 50mm(a), 48mm(b) and 46mm(c).

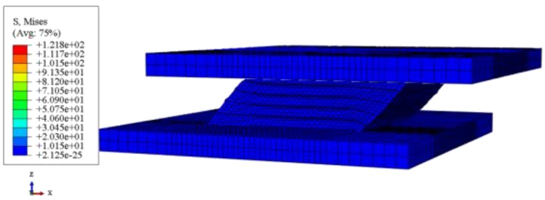

(a)

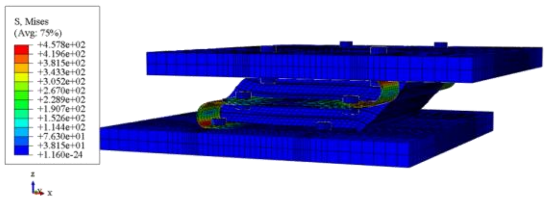

(b)

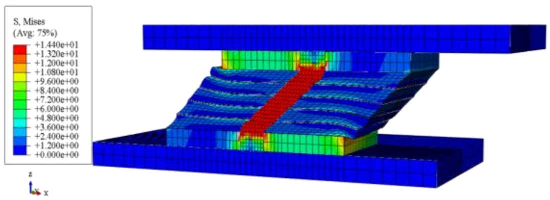

(c)

Figure 5: Mises stress distributions of SI (a), NHSI (b) and LRB (c) under cyclic shear test of 50mm.

5 CONCLUSIONS

From simulations results, it can be deduced that the numerical models with decreasing shape factors provide higher damping ratios and longer horizontal period. Typically, a seismic isolator alone (SI) has a low damping ratio, nearly 1%, and a horizontal period of approximately 1s.

The damping ratios of NHSI and LRB can reach up to 10%, which is ten times higher than that of a SI. However, as expected, the horizontal period of a SI is slightly longer than those of the other two isolators due to the contribution of steel dampers to the horizontal stiffness. Therefore, adding steel dampers can significantly enhance the energy dissipation capacity while maintaining effective energy isolation performance.

From the numerical analyses carried out for the different isolators, a dissipation device added in a traditional isolation system can enlarge considerably the hysteresis curve. LRB, including a lead core, is characterized by high cost and toxicity, even if it provides much more dissipation energy capacity.

The comparisons between NHSI and LRB shows that their effective horizontal stiffness and damping ratio are very close. It is possible to substitute a LRB with a NHSI to save money, at the same time maintaining the same efficient energy dissipation and an easy fabrication. Therefore, it can be concluded that the application of SSSDs in base isolation systems could dissipate energy properly and mitigate potential structural damage.

ACKNOWLEDGEMENTS

The author, Kai Guo, studies in Politecnico di Milano in Italy and would like to acknowledge China Scholarship Council to support his PhD program.

REFERENCES

[1] Habieb AB, Milani G, Cerchiaro R, Quaglini V, Milani F. Numerical study on rubber compounds made of reactivated ethylene propylene diene monomer for fiber reinforced elastomeric isolators. Polym Eng Sci 2021; 61:258–77. https://doi.org/10.1002/pen.25573.

[2] Habieb AB, Valente M, Milani G. Hybrid seismic base isolation of a historical masonry church using unbonded fiber reinforced elastomeric isolators and shape memory alloy wires. Eng Struct 2019; 196. https://doi.org/10.1016/j.engstruct.2019.109281.

[3] Haeri A H, Badamchi K, Tajmir Riahi H. Proposing a new hybrid friction yielding elastomeric bearing. JVCJournal Vib Control 2019; 25:1558–71. https://doi.org/10.1177/1077546319829535.

[4] Saadatnia M, Riahi HT, Izadinia M. The effect of cyclic loading on the rubber bearing with slit damper devices based on finite element method. Earthq Struct 2020; 18:215–22. https://doi.org/10.12989/eas.2020.18.2.215.

[5] Guo K, Milani G. Investigation of advanced seismic base isolation system using different shaped steel damper. AIP Conference Proceedings 2849, 420004 (2023).

[6] Guo K, Pianese G, Milani G. Finite element model for rubber seismic isolation with and without S-shaped steel dampers. COMPDYN Proc., National Technical University of Athens; 2023, p. 1–13.

[7] Kelly JM. The current status of seismic isolation technology in the United States. International Atomic Energy Agency (IAEA): 1992.
[8] Tsai H C, Kelly JM. Stiffness analysis of fiber-reinforced rectangular seismic isolators. J Eng Mech 2002; 128:462–70.
[9] Abaqus/Standard User's Manual, Version 6.14.